Materials Letters 64 (2010) 1476–1479

Contents lists available at ScienceDirect

Materials Letters

journal homepage: www.elsevier.com/locate/matlet

New material for orthopedic implants: Electrochemical study of nickel free P558 stainless steel in minimum essential medium

Ruth Flavia Vera Villamil Jaimes [a,*], Mónica Luisa Chaves de Andrade Afonso [b], Sizue Otta Rogero [c], Silvia Maria Leite Agostinho [d], Celso Antonio Barbosa [e]

[a] Universidade do Grande ABC, UniABC, Av. Industrial 3.330, Santo André, SP, Brazil
[b] Instituto Tecnológico e Nuclear, Unidade de Química do Estado Sólido, Estrada Nacional 10, 2686-953 Sacavém, Portugal
[c] Instituto de Pesquisas Energéticas e Nucleares, Av. Prof Lineu Prestes, 2242, 05508-000 São Paulo, SP, Brazil
[d] Instituto de Química, Universidade de São Paulo, Av. Prof. Lineu Prestes, 748, 05508-900 São Paulo, SP, Brazil
[e] Villares Metals S.A., Av Alfredo Dumont Villares, 155, 13178-902 Sumaré, SP, Brazil

ARTICLE INFO

Article history:
Received 8 September 2009
Accepted 30 March 2010
Available online 10 April 2010

Keywords:
Metals and alloys
Characterization methods
Corrosion
Nickel free P558 stainless steel
Minimum essential medium
Orthopedic implants

ABSTRACT

Nickel, a component of stainless steels (SS) applied in orthopedic implants may cause allergic processes in human tissues. P558 nickel free SS was studied to verify its viability as a substitute for stainless steel containing nickel. Its performance is compared to ISO 5832-9 and F138 most used nowadays grades in implants fabrications, in minimum essential medium, MEM, at 37 °C. Potentiodynamic polarization curves, electrochemical impedance spectroscopy (EIS), scanning electron microscopy (SEM) and "in vitro" cytotoxicity were used as techniques. From the electrochemical point of view P558 SS is comparable to ISO 5832-9 SS in MEM. It remains passivated until the transpassivation potential, above which generalized corrosion occurs. F138 presents pitting corrosion at 370 mV/SCE. The cytotoxicity results showed that P558, ISO 5832-9 and F138 do not present cytotoxic character. Therefore, these results suggest that P558 SS can be applied in orthopedic implants.

1. Introduction

There are basically three categories of metallic materials used in orthopedic implants: cobalt and titanium alloys and stainless steels (SS). Stainless steels are employed in surgical implants since 1936 [1–3]. The standard AISI 316 L has been used as a material for surgical implant applications for many years and it has demonstrated good biocompatibility, adequate physical and mechanical properties and it can be conformed into a variety of shapes and sizes [4–6]. The observed changes on the electrochemical behavior of Fe–Cr–Ni alloys have been often related to changes on the composition and structure of the passive film [7,8]. The ASTM F138 SS (ISO5832-1) was developed in 1970 in order to substitute 316 L SS [9]. In 1992 [10] a new steel, grade ISO 5832-9 (ASTM 1586-95 SS), was introduced as an orthopedic implant material. A new alloy, nickel free P558 SS, has recently been developed and studied for biomedical applications [11–13], because nickel may cause allergic reaction on tissues. This nickel free austenitic stainless steel presents both high N and Mn contents to stabilize the austenitic microstructure. Furthermore the higher N content promotes the improvement of the corrosion resistance thanks to its effects on the PREN-Pitting Resistance Equivalent Number [11].

In this work, P558 nickel free SS was studied in order to compare its electrochemical performance to both ISO 5832-9 SS and ISO 5832-1 SS in minimum essential medium (MEM), at 37 °C and to verify its cytotoxicity.

2. Experimental procedure

The chemical composition of the SS samples studied is given below. P558 SS: 16.50Cr-3.30Mo-0.48N-9.90Mn-0.40Si-0.18C; ASTM F 1586-95 (ISO 5832-9) SS: 20.70Cr-9.94Ni-2.50Mo-0.32N-0.28Nb-4.09Mn-0.014P-0.005S-0.33Si-0.015C; ASTM F138-92: 17.60Cr-14.20Ni-2.08Mo-0.021N-1.94Mn-0.023P-0.002S-0.26Si-0.012C. The PRE number (Pitting Resistance Equivalent) was calculated according to a previous work [11], using the equation: PRE = %Cr + 3.3% Mo + 16% N. The following PRE numbers were obtained: 35.3; ASTM F 1586-95 and ASTM F138-92:24.8.

The SS disk working electrodes were taken out from the central part of the bars and had an area of 0.32 cm^2. A cylindrical polytetrafluoroethylene (PTFE) sleeve was fitted with the steel disk. A concentric brass rod was coupled to the steel + PTFE. The surface treatment of these electrodes was described elsewhere [7]. A platinum foil with large area was used as counter electrode and the saturated calomel electrode as reference electrode. The composition of the electrolyte MEM was reported in previous papers [13]. The potentiodynamic polarization

* Corresponding author. Tel.: +55 11 4991 9824.
E-mail address: ruthflavia@uniabc.br (R.F.V.V. Jaimes).

0167-577X/$ – see front matter © 2010 Elsevier B.V. All rights reserved.
doi:10.1016/j.matlet.2010.03.066

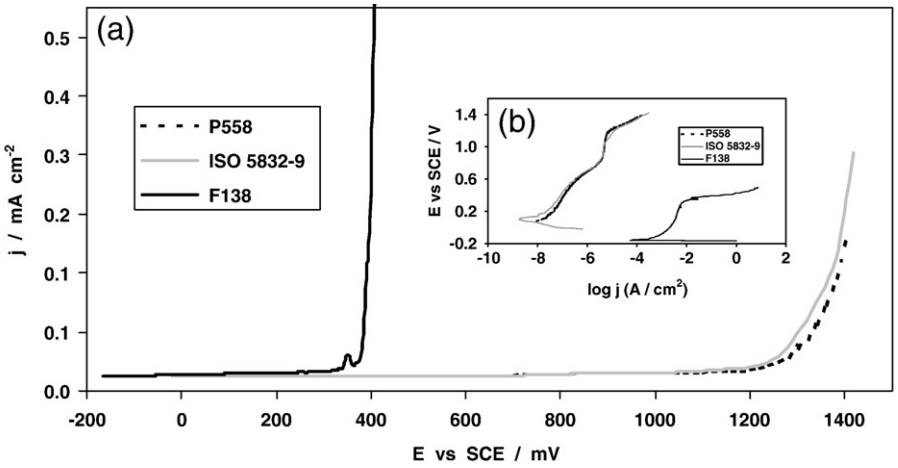

Fig. 1. Potentiodynamic polarization curves of SS in MEM solutions at 37 °C. (Fig. 1(a)). Fig. 1(b) shows the same electrochemical behavior using *E vs.* log *j*.

anodic curves were obtained for the studied SS in MEM at 37 °C using 0.17 mV s^{-1} scan rate starting from E_{corr}. The impedance measurements were performed over eight frequency decades (from 10.000 kHz to 5 mHz). The potential amplitude was ±8 mV, p.p. The experiments were conducted at 37 °C. A μAutolab type III/FRA2 potentiostat was used coupled to a Frequency Response Detector and to a

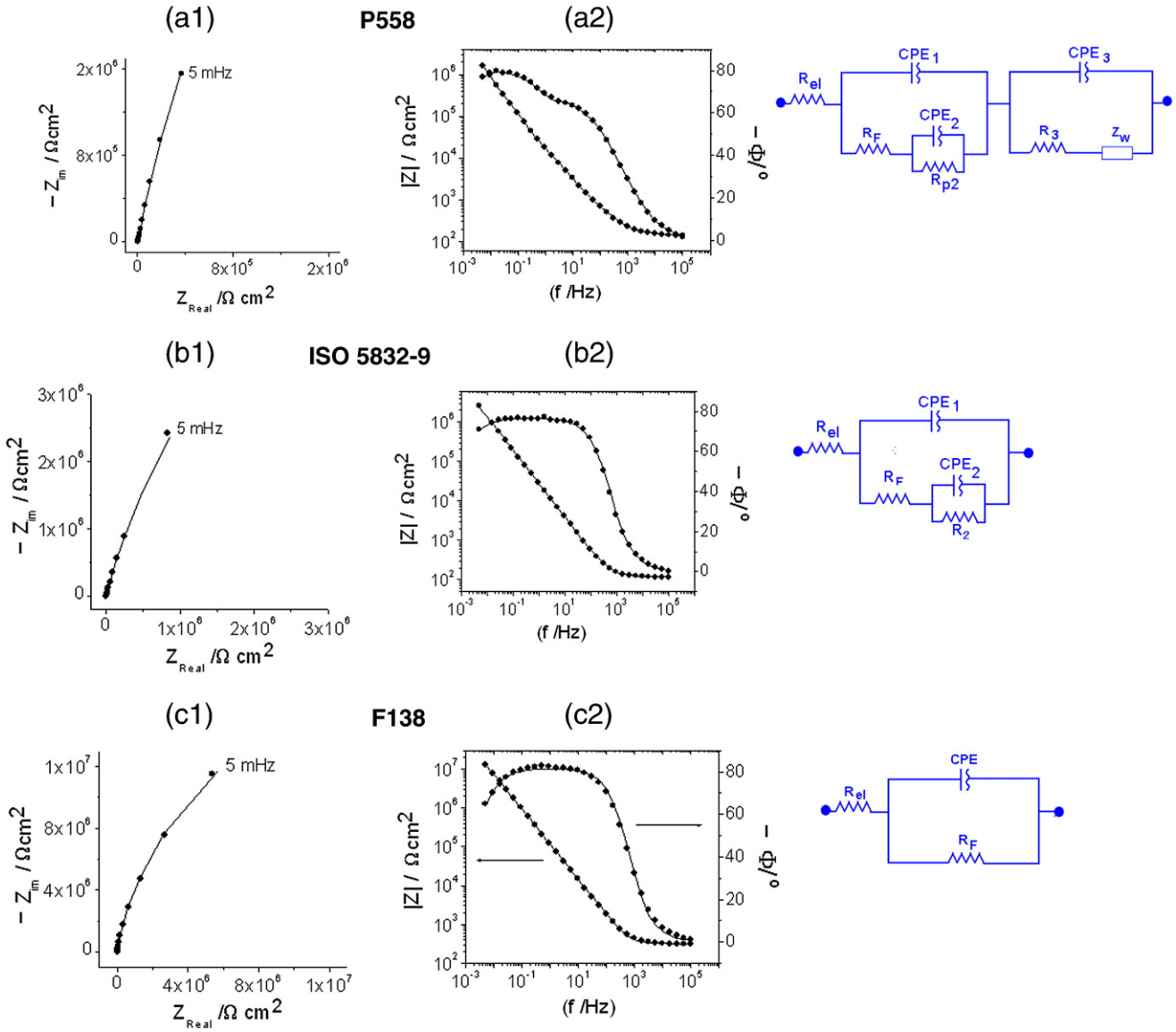

Fig. 2. Impedance spectra of SS in MEM medium at 37 °C. (1) Nyquist and (2) Bode plots.

microcomputer. SEM and EDS experiments were acquired on a WDX 600 Oxford microscope coupled to a Sterioscan 440 Leica. The samples were polished using 1 μm diamond paste, rinsed with water and ethanol and air dried. Previously to these experiments, the electrodes were immersed in the electrolyte and a constant potential was applied, at a value 50 mV higher than the potential of increase of the current (breakdown potential [11]) for 15 min. Different surface regions were analyzed using EDS. The procedure was adopted in order to guarantee an effective attack. The cytotoxicity assay was carried out with the exposure of the cell culture to the eluate obtained from samples, which stayed immersed for 10 days in culture medium MEM at 37 °C. The used cell line NCTC clone 929 was acquired from American Type Culture Collection (ATCC) bank. The cytotoxic effect was evaluated by neutral red uptake methodology (NRU), described in previous papers [14,15], according to the International Standard Organization [16].

3. Results and discussion

Fig. 1 presents the potentiodynamic polarization curves obtained from corrosion potential (−17 mV/SCE for P558, −20 mV/SCE for ISO 5832-9 and −165 mV/SCE for F138 SS).

It can be seen from Fig. 1 that F138 presents an abrupt increase of current density values near 300 mV *vs.* SCE suggesting the presence of pitting corrosion, while nickel free P558 and ISO 5832-9 remain passivated until the transpassivation potential. This potential value of the current increase corresponds to the occurrence of generalized corrosion (1350 mV for P558 and 1260 mV for ISO 5832-9SS). The passivation current densities (j_{pass}) obtained for nickel free P558, ISO 5832-9 SS and F138 SS, taken from the polarization curve data are respectively equal to (0.003 μA/cm^2, 0.01 μA/cm^2 and 3 μA/cm^2. E_i values were obtained graphically from the intersection of the two linear regions of the curves. It can be seen that nickel free P558 and ISO 5832-9 present lower passivating current densities than F138, suggesting a more protected surface in the passivation region for the first stainless steels cited. These results can be attributed to the lower nitrogen content of F138 SS [11].

Fig. 2 shows the electrochemical impedance spectroscopy results obtained at the open circuit potential. Nyquist diagrams are typical of passive systems with high values of both real and imaginary parts of the impedance at low frequencies. Further, the shape of Nyquist diagrams point out to different passivated surfaces. The evidence of arc profile increases in the sequence P558 SS (Fig. 2(a1)), ISO 5832-9 SS (Fig. 2(b1)) and F138 SS (Fig. 2(a1)–(c1). Bode phase diagrams also point out to different mechanisms: for nickel free P558 SS (Fig. 2(a2)) one can observe the presence of two waves. A broad plateau can be seen for ISO 5832-9 SS (Fig. 2(b2)) and F138 SS (Fig. 2(c2)). It is also shown in Fig. 2 the fitting of the experimental results according to simulated equivalent circuits. It is observed a good concordance between the experimental results and the equivalent circuits proposed, on the entire range of frequencies studied, suggesting qualitatively three distinct mechanisms where the complexity of the surface increases in the order F138, ISO 5832-9, P558 SS[12,13].

It can be seen from Fig. 3(a1) and (a 2) that the nickel free P558 SS presents after attach a surface similar to that observed after polishment without evidence of any kind of localized corrosion. Region 1 corresponds to the presence of an aluminum and magnesium oxides inclusion (a1), with a low Cr, Mn, and Fe percentage due to the higher penetration of the MEV probe compared to the inclusion diameter. Fig. 3(b1) and (b2)

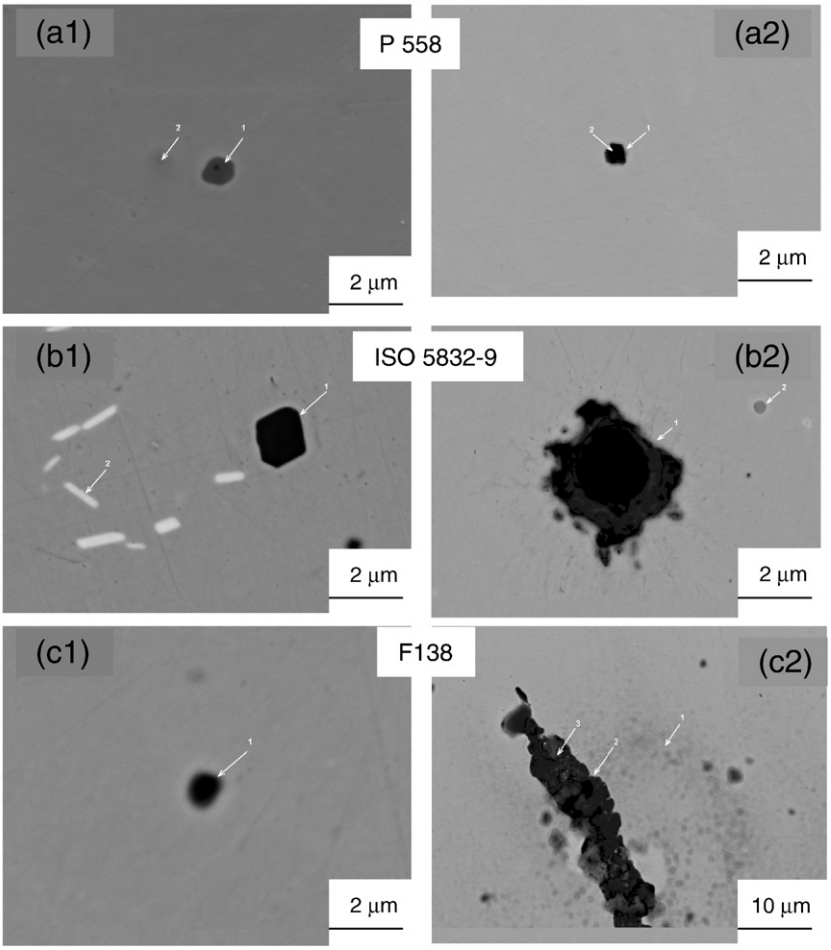

Fig. 3. SEM and EDS images of SS samples polished through 1 μm diamond paste (a1, b1, c1) and after attack (a2, b2, c2).

Table 1
Different surface regions analyzed using energy dispersive spectroscopy (EDS).

	After polishment							After attack in MEM									
	P558		ISO 5832-9			F138		P558			ISO 5832-9			F138			
	Bulk	1	Bulk	1	2	Bulk	1	Bulk	1	2	Bulk	1	2	Bulk	1	2	3
Cr	16.88	6.14	22.94	20.53	38.95	19.04	4.62	16.77	16.16	7.24	20.11	21.00	20.12	19.32	18.01	16.68	7.28
Mn	10.26	8.17	4.47	12.27	2.26	2.33	0.40	9.63	9.27	5.27	4.01	4.11	3.39	0.44	0.21	0.67	0.85
Ni	–	–	9.26	0.17	1.93	13.29	2.56	–	0.16	0.04	10.08	10.71	9.99	16.94	13.70	14.56	0.87
Nb	–	–	0.07*	0.02*	35.63	–		0.37	0.25	–	0.42	–	3.13	–	–	0.24	–
Si	0.48	0.08*	0.55	–	0.25*	0.54	0.33	0.42	0.16	–	0.34	0.28	0.14	0.37	0.30	0.39	0.25
S	–	–	–	–	–		0.40	–	0.09	0.27	–	0.25	–	–	0.36	0.08	0.69
Mo	3.35	0.73	1.70	–	–	1.33	–	3.23	2.91	1.24	2.24	1.37	2.34	5.49	4.07	4.60	0.64
O	–	34.19	–	61.7	–		51.56	2.20	6.11	31.63	3.05	1.83	4.88	4.07	13.10	12.12	42.58
Al	–	25.34	–	3.04	–	–	26.40	–	3.97	29.44	0.12	0.15	0.08	0.11	–	1.82	21.71
Ti	–	–	–	1.15	–	–	–	–	–	–	–	–	–	–	–	–	–
V	–	–	–	–	0.65	–	–	0.07	0.06	0.12	–	–	0.10	0.23	–	0.08	0.13
Cl	–	–	–	–	–	–	–	0.10	0.09	–	0.16	0.22	0.10	–	–	0.11	0.77
Mg	–	6.39	–	–	–	–	–	–	–	0.44	0.22	–	0.06	0.08	0.07	0.28	0.04
Ca	–	–	–	–	–	–	–	0.01	0.15	3.04	0.02	0.02	0.07	0.14	0.17	0.61	11.68
P	–	–	–	–	–	–	–		0.11	0.04	0.05	–	–	0.28	1.16	0.60	3.75
Fe	69.03	18.96	61.02	0.99	20.34	63.45	13.72	67.19	60.48	21.23	59.18	60.06	55.60	52.54	48.88	47.16	8.78

point out to a similar bulk surface of ISO 5832-9 SS with the attack promoting the partial dissolution of inclusions (regions 1 — Mn and Al oxides and 2 — Nb and Cr carbides). This is supported by the EDS results listed in Table 1 where it can be seen that, after the electrochemical attack only trace amounts of Mn, Al and Nb are detected. Further, the presence of chlorine on the entire surface denotes the generalized attach. Fig. 3(c1) and (c2) show that the surface of the F138 SS (bulk composition) is the same after polishment and after attach in MEM. Regions 1 and 2 correspond to aluminum oxide inclusion. It is interesting to note the presence of high molybdenum content on the surface after attach (bulk, regions 1 and 2). Region 3 correspond to aluminum and calcium oxides inclusions and after attach presents a relative quantity of chlorine and calcium from the electrolyte as an indicative of pitting formation around the inclusions.

Fig. 4 shows the cytotoxicity evaluation performed by neutral red uptake assay. Positive and negative controls were used to confirm the adequate performance of the test procedure and/or to evaluate the results from a new material, as well as to control cell sensitivity, extraction efficiency, and other test parameters. The sample that present cell viability curve above the $IC_{50(\%)}$ line is considered non-toxic and under $IC_{50(\%)}$ line is extremely toxic. In this study the tested samples did not present toxic effects even at 100% extract concentration. P558, ISO 5832-9 and F138 SS demonstrated similar behavior to negative control with no cytotoxic effect as shown in Fig. 4. All the viability curves are above the cytotoxicity index line, which means that all the samples showed no cytotoxicity in this assay.

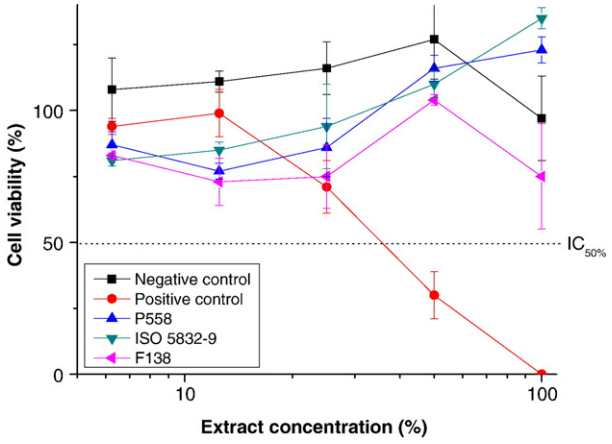

Fig. 4. SS viability curves in the cytotoxicity assay by the neutral red uptake methodology.

4. Conclusions

The results have shown that nickel free P558 presents electrochemical behavior comparable to ISO 5832-9 steel in MEM. P558 SS shows only generalized corrosion at 50 mV above the transpassivation potential. F138 steel shows pitting corrosion around the inclusions. The materials studied, nickel free P558, ISO 5832-9 and F138 SS, do not present cytotoxic character. These results suggest, therefore, that nickel free P558 SS under the electrochemical and cytotoxicity point of view can be used as biomaterials to be applied in orthopedic implants. The biocompatibility study has to be continued according to International Standard Organization.

Acknowledgements

The authors would like to thank to Conselho Nacional de Desenvolvimento Científico e Tecnológico (CNPq) for financial support.

References

[1] Mears DC. Review 218. Int Met Rev 1977:119–55.
[2] Fraker AC, Ruff AW. J Met 1977:22–8.
[3] Gotman I. J Endourol 1997;11(6):383–9.
[4] Reclaru L, Lerrf R, Eschler PY, Meyer JM. Biomaterials 2001;22:269–306.
[5] Villamil RFV, Aranha H, Afonso MLCA, Mercadante MT, Agostinho SML. Rev Bras Ortop Traumatol 2002;37:471–6.
[6] Basridas JM, Polo JL, Torres CL, Cano E. Corr Sci 2001;43:269.
[7] Afonso MLCA, Villamil Jaimes RFV, Arêas EPG, Capri MR, Oliveira E, Agostinho SML. Colloids Surf A: Physicochem Eng Aspects 2008;317:760–3.
[8] Fini M, Nicoli AN, Torricelli P, Giavaresi G, Borsari V, Lenger H, Bernauer J, Giordano R, Chiesa R, Cigada A. Biomaterilas 2003;24:4929–39.
[9] ASTM Designation F138–92 Standard Specification for Stainless Steel Bar and Wire for Surgical Implants (special Quality).
[10] International Standard ISO 5832-9. Implants for Surgery-Metallic Materials- part 9: Wrought high nitrogen stainless steel.
[11] Villamil RFV, Andrade AHP, Barbosa CA, Sokolowski A, Agostinho SML. In: Winters GL, Nutt MJ, editors. Stainless Steels for Medical and Surgical Applications, ASTM STP 1438; 2003. p. 168–75. West Conshohocken, PA.
[12] Rondelli G, Torricelli P, Fini M, Giardino R. Biomaterials 2005;26:739–44.
[13] Jaimes RFVV, Afonso MLCA, Agostinho SML, Barbosa CA. REM 2007;60(1):63–8.
[14] Rogero SO, Hilga OZ, Saiki M, Correia OV, Costa I. Toxicol In Vitro 2000;14(6): 497–504.
[15] Ossa CPO, Rogero SO, Tschiptschin APJ. J Mater Med 2006;17(11):1095–100.
[16] ISO document 10993-5. Biological evaluation o medical devices, part 5. Test for cytotoxicity: in vitro methods; 1992.